Highlights of Spanish Astrophysics VIII, Proceedings of the XI Scientific Meeting of the Spanish Astronomical Society held on September 8–12, 2014, in Teruel, Spain. A. J. Cenarro, F. Figueras, C. Hernández-Monteagudo, J. Trujillo Bueno, and L. Valdivielso (eds.)

Studies of short-period comets on the eve of Rosetta

F. J. Pozuelos[1], F. Moreno[1], F. Aceituno[1], V. Casanova[1], A. Sota[1], J. J. López-Moreno[1], and Cometas-Obs Team[2]

[1] Instituto de Astrofísica de Andalucía (CSIC), Glorieta de la Astronomía s/n, 18008 Granada, Spain
[2] Astronomy Amateur Association, Spain

Abstract

We present an extended study of the dust environment of a sample of short-period comets and their dynamical history. With this aim, we characterized the dust tails when the comets are active, and we make a statistical study to determine their dynamical evolution. The targets selected were 22P/Kopff, 30P/Reinmuth 1, 78P/Gehrels 2, 81P/Wild 2, 103P/Hartley 2, 115P/Maury, 118P/Shoemaker-Levy 4, 123P/West-Hartley, 157P/Tritton, 185P/Petriew, P/2011 W2 (Rinner).

1 Introduction

Cometary science has been revolutionized by *in situ* missions over the last decades. It will continue to develop and transform with the arrival of Rosetta Spacecraft at the comet 67P/Churyumov-Gerasimenko. The comet 67P/C-G is a short-period comet, which belongs to the Jupiter Family. Thus, in this work we present our latest results obtained to this kind of objects. These results have been published in [6, 7, 8].

2 Methods

The analysis we have done consists of two different parts: the first one is a dust characterization using our Monte Carlo dust tail code. This procedure allows us to derive the dust parameters: mass loss rates, ejection velocities, and size distribution of the particles (i.e. maximum size, minimum size, and the power index of the size distribution). The second part in our study is the analysis of the recent (15 Myr) dynamical history for each target. To perform this task, we use the numerical integrator developed by [2]. This will serve to derive the time spent by each comet in each region and, specifically, in the Jupiter Family region, where it supposed that the comets become active periodically. For further details we refer the readers to [6, 7, 8].

3 Results

Due to the large number of targets studied in this work, we only present here a representative example. Thus, we focus on the results obtained to 81P/Wild 2. This comet is of special interest as target of the spacecraft mission Stardust. This comet has an effective nucleus of $R_{\rm N} = 2.00\,\mathrm{km}$ [9] and a bulk density of $\rho = 600\,\mathrm{kg\ m^{-3}}$ reported by [3]. Our observational data for comet 81P are six direct images post-perihelion passage at OSN 1.52 m telescope and ~ 300 $Af\rho$ measurements by *Cometas-Obs*, which cover from ~ -2.15 to ~ 2.45 AU. In addition, we benefited from observations carried out in the 1 m Lulin telescope by Z.-Y. Lin. From these observations we selected one pre-perihelion image (January 16.81, 2010) and 5 $Af\rho$ measurements pre- and post-perihelion.

3.1 Dust analysis

We observed two enhancements in the measurements that were not related to low phase angles values. We considered them as small outbursts suffered by the comet. The first one occurred on October 29 (2009), when the comet was at $r_h \sim 1.949$ AU inbound, where the maximum value of $Af\rho$ was ~ 782 cm. To our knowledge, this outburst has not been reported previously. In our dust characterization we concluded that the event duration was ~ 40 h, and the comet emitted $m_{ob.I} \sim 9.2 \times 10^8$ kg of dust, reaching a peak dust production rate of $1190\,\mathrm{kg\ s^{-1}}$, returning to normal activity on November 13. However we only have a limited number of sample observations for this period, so this result must be read with caution. The second outburst was first identified by [1]. This second event took place post-perihelion, August 5 (2010), at ~ 2.215 AU outbound, with a maximum value of $Af\rho \sim 380$ cm. Our dust analysis estimated this event as three times less intense than the first one, $m_{ob.II} \sim 3.0 \times 10^8$ kg with a duration of ~ 55 h and a peak dust production rate of $450\,\mathrm{kg\ s^{-1}}$. During both outbursts, I and II, the maximum particle size was 3 cm.

Overall, without taking the outburst events into account, we concluded that the comet reached its maximum level of activity at $r_h \sim 1.64$ AU inbound, that is ~ 40 days before perihelion, with a dust production rate of $900\,\mathrm{kg\ s^{-1}}$. The comet emission pattern is found to be anisotropic at 35%, with active areas located on the surface between $+45°$ to $-30°$. From the anisotropic model we derived the rotational angles as $I = (50 \pm 5)°$ and $\phi = (300 \pm 20)°$. In Fig. 1 we display the evolution of the dust parameters as a function of heliocentric distance, and in Figs. 2 and 3 we present the comparison of the model with the observational data, which are remarkably similar. From the dust analysis, we determined that the total dust production rate of 81P was 1.1×10^{10} kg during the 3.8 yr covered by the study, that is, an annual dust production rate of $T_d = 2.8 \times 10^9\,\mathrm{kg\ yr^{-1}}$ and an average dust mass lost rate of $87.5\,\mathrm{kg\ s^{-1}}$. The contribution to the annual interplanetary dust replacement, established by [4] as $2.9 \times 10^{11}\,\mathrm{kg\ yr^{-1}}$, is $\sim 0.96\%$.

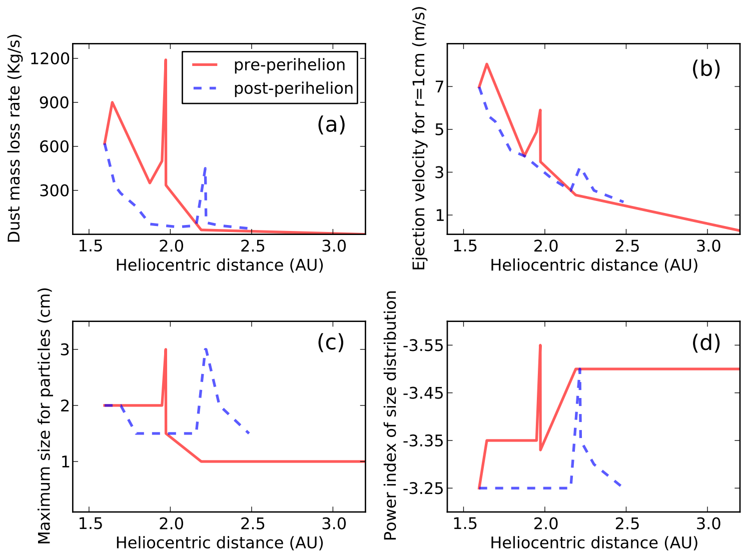

Figure 1: The best-fit modeled parameters to the dust environment of 81P/Wild 2 $Af\rho$ data and images (Fig. 2 and Fig. 3). All parameters are given as a function of the heliocentric distance. From top to bottom and left to right the panels are: (a) Dust production rate [kg s^{-1}]; (b) Ejection velocities of 1-cm particles [m s^{-1}]; (c) Maximum size of particles [cm]; (d) Power index of the size distribution, δ. The solid red line corresponds to pre-perihelion and the dashed blue line to post-perihelion.

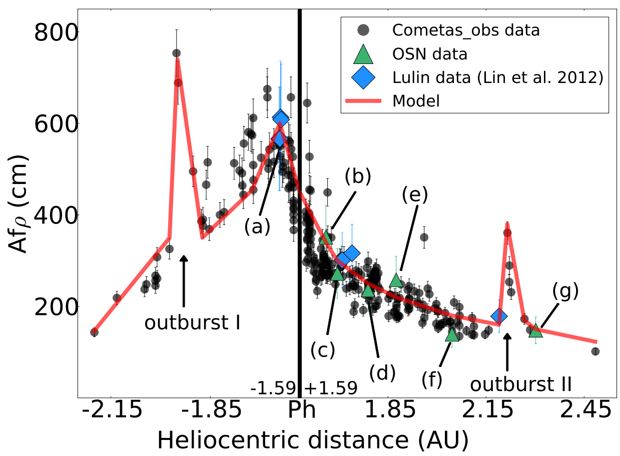

Figure 2: Comparison of observed and modeled $Af\rho$ data as a function of heliocentric distance. Black dots, $Af\rho$ data from *Cometas-Obs*. Green triangles, $Af\rho$ data derived from OSN images. Blue diamonds, $Af\rho$ data from Lulin observatory images. The observations labeled (a) to (g) correspond to the $Af\rho$ derived from images (a) to (g) in Fig. 3. The outbursts I (inbound) and II (outbound) described in the text are marked with arrows. All the $Af\rho$ values are referred to $\rho = 10^4$ km.

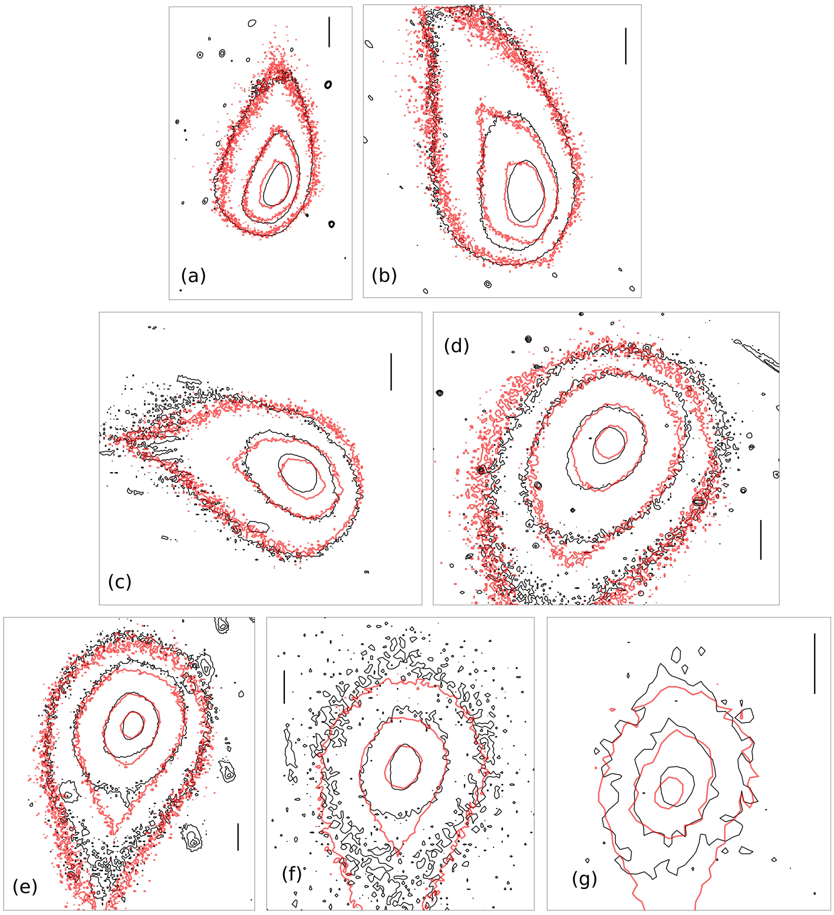

Figure 3: Isophote field comparison between observations and model. The black contours correspond to the observations and the red ones to the model. The dates are:(a) Jan 16.81, 2010; (b) Apr 9.06, 2010; (c) Apr 21.06, 2010; (d) May 15.96, 2010; (e) Jun 3.93, 2010; (f) Jul 6.89, 2010; (g) Aug 21.85, 2010.

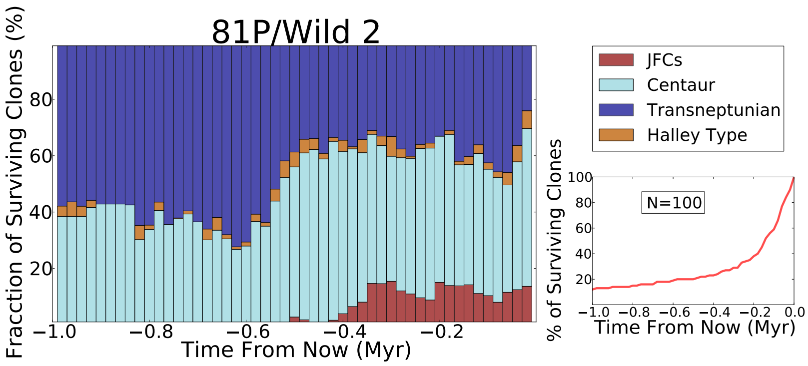

Figure 4: 81P/Wild 2 backward in time orbital evolution during 1 Myr. *Left panel*: fraction of surviving clones (%) versus time from now (Myr). The colors represent the regions visited by the test particles (red: Jupiter Family region; cyan: Centaur; blue: Transneptunian; yellow: Halley Type). The resolution is 2×10^4 yr. *Right bottom panel*: the % of surviving clones versus time from now (Myr), where N = 100 is the number of the initial test massless particles.

3.2 Dynamical history analysis

In order to obtain the dynamical evolution of this comet, we followed the previous studies by [5]. We use version 6.2 of the Mercury's numerical integrator developed by [2]. We generated 99 clones having 2σ dispersion in the three of the orbital elements: semimajor axis, a, inclination, i, and eccentricity, e, where σ is the uncertainty in the corresponding parameter as given in the JPL Horizons on-line Solar System data (see ssd.jpl.nasa.gov/?horizons). The 99 clones plus the real object make a total of 100 massless particles to perform the statistical study. The Sun and the 8 planets are take into account as massive bodies. To control the close encounters of the massless particles to the massive bodies, we used the hybrid algorithm which combines a symplectic algorithm with a Burlisch-Stoer integrator. The initial time step was 8 days, and the clones are removed when their heliocentric distance is > 1000 AU. We performed backward integrations of 15 Myr, where the non-gravitational forces were neglected.

After the analysis of the 15 Myr integration, we focused on the first 1 Myr of backward in the orbital evolution, where $\sim 20\%$ of the massless particles still remained in the Solar System. We inferred that 81P has a Centaur and Transneptunian past, while Halley Type region was the most unlikely source for this comet, as expected (see Fig. 4). After that, in order to obtain the time spent in the JFCs region, we displayed the last 100 yr with a 3 yr temporal resolution, and we found that 81P has ~ 40 yr in this region (see Fig. 5).

4 Summary and conclusions

In this work we present an accurate characterization of the dust parameters which best describe the dust environment of the comets during a significant orbital arc around their perihelion passages. These parameters are: dust loss rates, size distribution functions of the

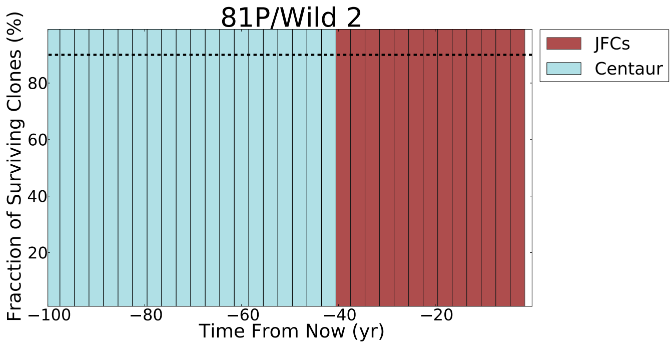

Figure 5: 81P/wild 2 last 100 yr. fraction of surviving clones (%) versus time from now (yr). The colors represent the regions visited by the test particles (red: Jupiter Family region; cyan: Centaur). The dashed line marks the bars with a confidence level equal or larger than 90% of the clones in the Jupiter Family region. The resolution is 3 yr, and the number of the initial test particles is N = 100.

particles, ejection velocities, and the emission patterns. To this end, we use our Monte Carlo dust tail code. In addition, using the numerical integrator Mercury 6.2 developed by [2], we have determined the dynamical history of each comet, in order to identify the Solar System regions visited and the time spent there, for each comet. From these two different analyses, we relate the annual dust production rate with the time spent in the region of JFCs for all comets. The main result obtained, is that the highly active comets are also the youngest ones with age in the range of $40 - 600$ yr in the Jupiter Family region.

References

[1] Bertini, I., Barbieri, C., Ho, T.-M., et al. 2012, A&A, 541, A159

[2] Chambers, J. E. 1999, MNRAS, 304, 793

[3] Davidsson, B. J. R. & Gutierrez, P. J. 2004, in Bulletin of the American Astronomical Society, Vol. 36, AAS/Division for Planetary Sciences Meeting Abstracts 36, 1118

[4] Grun, E., Zook, H. A., Fechtig, H., et al. 1985, Icarus, 62, 244

[5] Levison, H. F. & Duncan, M.J. 1994, Icarus, 108, 18

[6] Moreno, F., Pozuelos, F. J., Aceituno, F., et al. 2012, ApJ, 752, 136

[7] Pozuelos, F. J., Moreno, F., Aceituno, F., et al. 2014, A&A, 568, A3

[8] Pozuelos, F. J., Moreno, F., Aceituno, F., et al. 2014, A&A, 571, A64

[9] Sekanina, Z., Brownlee, D. E., Economou, T. E., et al. 2004, Science, 304, 1769